International Journal of
Water and Wastewater Treatment
ISSN 2381-5299 | Open Access

RESEARCH ARTICLE

Volume 4 - Issue 1 | DOI: http://dx.doi.org/10.16966/2381-5299.153

Adsorption of Mn^{2+} from the Acid Mine Drainage using Banana Peel

Jan Mbongeni Mahlangu[1,2]*, Geoffrey S Simate[1] and Marinda de Beer[2]

[1]*School of Chemical and Metallurgical Engineering, University of Witwatersrand, South Africa*
[2]*DST/CSIR National Centre for Nanostructured Materials, Council for Scientific and Industrial Research, South Africa*

***Corresponding author:** Jan Mbongeni Mahlangu, School of Chemical and Metallurgical Engineering, University of Witwatersrand, South Africa, **E-mail:** janmbn@gmail.com

Received: 28 Jun, 2018 | **Accepted:** 25 Jul, 2018 | **Published:** 31 Jul, 2018

Citation: Mahlangu JM, Simate GS, de Beer M (2018) Adsorption of Mn^{2+} from the Acid Mine Drainage using banana peel. Int J Water Wastewater Treat 4(1): dx.doi.org/10.16966/2381-5299.153

Abstract

The sustainable removal of heavy metals from Acid Mine Drainage (AMD) has become a major challenge to scientists and engineers despite numerous treatment technologies. This is because most of the explored technologies are too expensive and also have significant disposal challenges. Therefore, the need to develop a more effective and affordable technology for the removal of heavy metals from AMD is inevitable. The banana peel, the most abundant fruit that is almost consumed across the world, was explored in this study to evaluate its potential to remove heavy metals under AMD conditions. The adsorption of manganese metal ion (Mn^{2+}) has been studied to investigate the effects of controlling parameters such as particle size, doses, and initial concentration of Mn^{2+}, contact time, pH and selectivity of the banana peel. Synthetic single component solution and actual AMD were used in a batch system. Langmuir and Freundlich isotherms were applied to describe adsorption equilibrium. The maximum amount of Mn^{2+} metal ions adsorbed, as evaluated by Langmuir isotherm was 6.920 $mg.g^{-1}$. The adsorption data also fitted the pseudo second order kinetics very well and suggested that the adsorption is characterized by the valence forces through exchange of charges between banana peel powder and heavy metal ion.

Continuous fixed bed column studies were conducted by using AMD at room temperature and the effects of various parameters like flowrate and bed depth were investigated. The column bed capacity and saturation time as expected increased with the increase of bed depth and decrease of flowrate. The results show that the column performed well at lowest flowrate. The Thomas model and Bed Depth Service Time (BDST) model were applied to evaluate the breakthrough curves and to analyse the experimental data. The results obtained in this study demonstrated that the banana peel powder can be used for the removal of Mn^{2+} ions from AMD using batch and fixed bed adsorption system.

Keywords: Acid mine drainage; Manganese ion; Banana peel; Adsorption

Introduction

Mining plays a major role in global economy in terms of employment and income generation particularly of emerging economies. In 2010 the global mining industry, including the quarrying and petroleum sectors, represented 11.5% of the world's gross domestic products, as measured by revenues from mining products sold [1]. Unfortunately, mining activities have triggered pollution of water, land sinking and air pollution. Basically, when water reacts with pyrite in the host rocks it releases heavy metals and becomes acidic [2]. This is termed Acid Mine Drainage (AMD). This leads to land sinking which lead to the surface cracking [3], erosion of soil and air pollution, and decrease of biodiversity [4]. Subsequently, the wellbeing of society and agricultural economy is threatened by the contamination of the soil and water by heavy metals due to the AMD.

In mitigation of ecological damages, conventional active treatment techniques are currently used to combat AMD effects [5]. These processes include neutralisation, oxidation and reduction, extraction, sedimentation and flocculation and ion exchange and precipitation [6]. However, these processes vary in cost and effectiveness [7] and have their short comings. For example, the techniques based on ion exchange, chemical or biological oxidation have shown low efficiency for removal of trace contaminants [8]. On the other hand, sedimentation and flocculation, and neutralisation techniques produce a bulk metal laden sludge that poses a disposal challenge.

Notwithstanding these treatment challenges, adsorption is one of the emerging technique used in removal of water contaminants, its simplified design and ease of operation makes it more superior than conventional methods of water treatment. It also eliminates the problem of sludge disposal and renders the system more feasible. This technique exploit surface phenomenon through application of surface forces and concentrating of the contaminants on the surface of the adsorbent [9]. Cellulosic agricultural waste used as adsorbents have shown potential to remove contaminants such as heavy metals

from wastewater [10], these types of adsorbents are mainly available as waste and are in abundant and cheap [11]. One of these cellulosic agricultural wastes is banana peel that is spread worldwide and has shown capability to remove heavy metals at significant capacity [12].

The objective of this study is to explore the adsorption potential of banana peel as low cost adsorbent for adsorption of Mn^{2+} from AMD.

Materials and Methods

Batch studies

Material preparation: Banana peels were collected from local supermarkets. The pith on the peel was removed and the peels were cut into small pieces (1-2 cm), washed with deionized water to remove external dirt and dried in an oven at 80°C for 24 hours. Thereafter, the peels were subjected to a crusher to reduce particle sizes, and then soaked into deionized water for 6 hours to remove the dissolved pigment that readily dissolves in water and dried again for 6 hours at 80°C. The banana peels used during the adsorption study were at natural state with no chemical or thermal treatment. The BET was used to study the surface area of the banana peels. The surface morphology and functional groups of the banana peels were studied before and after adsorption by Scanning Electron Microscope (SEM) and Fourier-Transform Infrared (FTIR) spectroscopy, respectively.

Chemicals: All the chemicals used in this work were of analytical grade and actual AMD was collected in four 25 L bottles from a decant point in Mpumalanga, South Africa. The synthetic solution stock solution of Mn^{2+} (1000 mg/L) was prepared by dissolving appropriate quantity of analytical grade of $MnSO_4.4H_2O$ in water at room temperature. The desired concentrations were prepared by successive dilutions of the stock solution.

Adsorbent particle size: The crusher and vibrating sieve were used for the reduction of particle size of the dried banana peel and for particle size distribution, respectively. The sieves were mechanically vibrated for 15 minutes which was sufficient for separation to take place. The screens were subjected to weighing balance before and after the vibration to get the mass and size of the banana peel particles retained on each sieve. The particle size range used in this study was 0.15 mm to 5 mm.

Effects of adsorbent particle size: The effects of adsorbent particle size on percentage removal of heavy metals were investigated. Four different particle sizes (dp=aperture size) were used; $0.08<dp<0.15$, $0.15 \leq dp \leq 0.4$, $0.4 \leq dp \leq 1$, and $1 \leq dp \leq 5$ mm. 1000 mg of adsorbent at the required particle size was mixed with 200 mL solution of the appropriate single component solution for (180 min) at room temperature (22°C) and samples were collected at regular intervals and analysed by Inductively-Coupled Plasma Mass Spectrometer (ICP-MS).

Effect of adsorbent mass: Six different masses were used in this study 200, 400, 600, 800, 1000 and 1200 mg of banana peels in 200 mL of solution. The mixture was agitated for 180 minutes and samples were taken at regular intervals (5, 10, 20, 30, 45, 60, 90, 180 minutes) for the analysis of metal ion concentrations by ICP-MS. The particles of the banana peels used were 0.4 mm.

Effect of initial solution pH: The solution pH was varied as follows: 2.0, 3.0 and 5 ± 0.2 for the Mn^{2+} synthetic solution. Solution pH was adjusted using 0.2 M H_2SO_4 and 0.1 M NaOH. The solution was put into the shaker bath for 180 minutes at room temperature (22°C). The pH of the solution was measured using pH meter.

Effects of initial solution concentration: The effect of initial metal concentration on the removal of Mn^{2+} from solution by banana peels was investigated by contacting 1000 mg of banana peel powder in a 200 mL of Mn^{2+} solution with concentration ranging (25 mg/L to 100mg/L). The experiments were run for 180 minutes.

Selectivity of the adsorbent: The AMD generally comprises of more than one cation, i.e., it is a mixture of different heavy metals as listed in table 1. Tests were performed to investigate the influence of the presence of other cations on the adsorption capacity of banana peels for heavy metals in actual AMD.

Column studies

Fixed bed column experiments were carried out in a laboratory scale Perspex columns with a fixed diameter of 3.5 cm and height of 50 cm. The column was fitted with a glass beads and glass wool at both ends to keep the adsorbent bed in a fixed position. The experiments were carried out to study the effects of bed depth and flowrate of the influent for the adsorption of Mn^{2+}. The concentration of Mn^{2+} in actual AMD solution was 46.01 mg/L, at the pH of 3.12. The range of the bed depth investigated was 6 to 17.8 cm at the fixed flowrate of 15 mL/min while the flowrate investigated ranges from 15 to 45 mL/min at the fixed bed depth of 17.8 cm. The samples of the treated actual AMD solution were collected from the upstream of the column at different time intervals and analysed using ICP-MS. The samples were collected and analysed until bed saturation was reached. The desired breakthrough concentration of the bed was 0.2% of the initial concentration of the AMD entering the bottom of the column.

Results and Discussion

Batch studies

Particle size distribution: The size distribution of the banana peel particle is shown in figure 1. 5 kg of banana peel particles were distributed on the mechanically vibrated sieve and particle size range (dp=particle diameter) of $0.15<dp<0.4$ mm was used for this study.

Surface area and porosity: The specific surface area of the banana peel adsorbent at different particle size listed in table 2 was less than 1 m^2/g. This range of surface area is in agreement with other studies on fruit peels [13]. The surface area of the particle size chosen for the study was 0.011 m^2/g.

Surface morphology and functional group of the banana peel powder: Scanning Electron Microscopy (SEM) was used as a tool for studying surface morphology and fundamental physical properties of the banana peel. The characterization of the banana peel powder before (Figure 2a) and after (Figure 2b) adsorption showed a change in the surface morphology of the adsorbent. Rough surface texture and porosity could be distinctly noticed after adsorption. Spent banana peel (Figure 2b) shows a less compacted surface of the banana peel than the original (Figure 2a) compacted surface.

Table 1: Heavy metals constituent of the AMD

Heavy metal ion	Concentration (mg/L)
Zn^{2+}	3.510
Mn^{2+}	46.006
Co^{2+}	3.18
Fe^{3+}	6.102
Ni^{2+}	3.750
Cd^{2+}	0.350
Al^{3+}	15.12

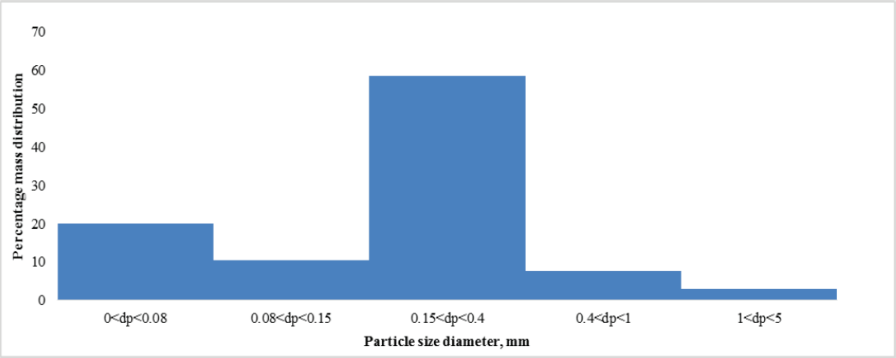

Figure 1: Particle size distribution of the banana peel

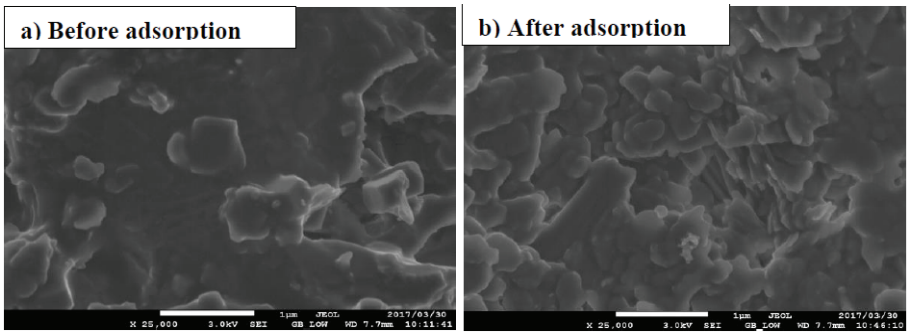

Figure 2: SEM images of the banana peel before (a) and after (b) adsorption

Table 2: Surface area of the banana peel particle size

Adsorbent	Particle size (mm)	BET surface area × 10^{-4}(m^2/g)
Banana peel	5	1.813
	1	6.010
	0.4	113.54
	0.15	121.42

The FT-IR spectra shown in figures 3a and 3b were obtained in order to understand the nature of the functional groups in the banana peel. The FTIR spectra in figures 3a and 3b shows a number of peaks, indicating the nature of the banana peel adsorbent. The peaks observed at 2920 cm^{-1} can be attributed to the C-H stretching alkane groups. Bands appearing at 1706, 1734, 1290, 1212, 1246, 1614,2852, 3020, and 3386 cm^{-1} in figures 3a and 3b were assigned to stretching carboxylic acid dimer, COO^- anion stretching, C-O stretching aromatic ester, stretching secondary alcohol, C-O stretching alky aryl ether, N-H stretching amine salt, O-H stretching alcohol, and N-H stretching aliphatic primary amine respectively. Hydroxyl and carboxylic acid played a key role in the removal of divalent metals Mn^{2+} ions. The peak observed at 1412 cm^{-1} in figure 3b is attributed to nitrates. It indicates that the banana peel has adsorbed the nitrates from the AMD. The adsorption of the metals did not change the position of the peaks but the intensity of the peaks for functional groups of the adsorbent has been reduced this may be due to the coverage of the surface of the banana peel by the adsorbed ions.

Effects of adsorbent dosage: A series of kinetic experiments at different adsorbent mass, that is, 200 mg, 400 mg, 600 mg, 800 mg, 1000 mg and 1200 mg were conducted using a fixed initial concentration for the respective metal. Typical plots of the amount of metal adsorbed as percentage removal are shown in figure 4. This figure 4, shows kinetic study conducted at different banana peel powder dosage, 200, 400, 600, 800, 1000, 1200 mg for 180 minutes, indicates that the sorption was quick, the saturation was reached within 60 minutes for all dosages, and is comparable to the results reported by [14,15] on adsorption of Mn^{2+} by agricultural waste. The results show that Mn^{2+} percentage removal increase with the increase in adsorbent dosage. In order to circumvent the error in the experiments, sorption time of 180 min was adopted for subsequent studies. The increase in percentage removal with adsorbent dosage can be attributed to an increase in adsorption sites per unit mass of adsorbent.

Effects of initial concentration: Figure 5 shows that percentage removal of Mn^{2+} decreased with increasing initial concentration. On initial concentration above 50 mg/L, Mn^{2+} adsorbed decreased from 62.61% to 43.14% respectively. This can be attributed to the increasing metal ions concentration with the constant active sites of the adsorbent. Adsorption capacity of the banana powder with respect Mn^{2+} at 50 mg/L has reached a saturation point with the optimum percentage removal of 70.58%. However, the amount of metal ions adsorbed per unit mass of banana peel increased with an increase in initial metal ion concentration this is in concordance with [16]. This increase could be due to an increase in electrostatic interactions relative to covalent interactions, involving sites of progressively lower affinity for metal ions [17].

Equilibrium adsorption isotherms: The fitting of Langmuir and Freundlich models to experimental data for the adsorption of Mn^{2+} is shown graphically in figures 3 and 4. Figure 3 shows that Langmuir isotherm for the adsorption of Mn^{2+} from solution gave good fit of the experimental results, as shown by the value of the correlation coefficient, R^2, which is 0.971 (Table 3). The maximum adsorption

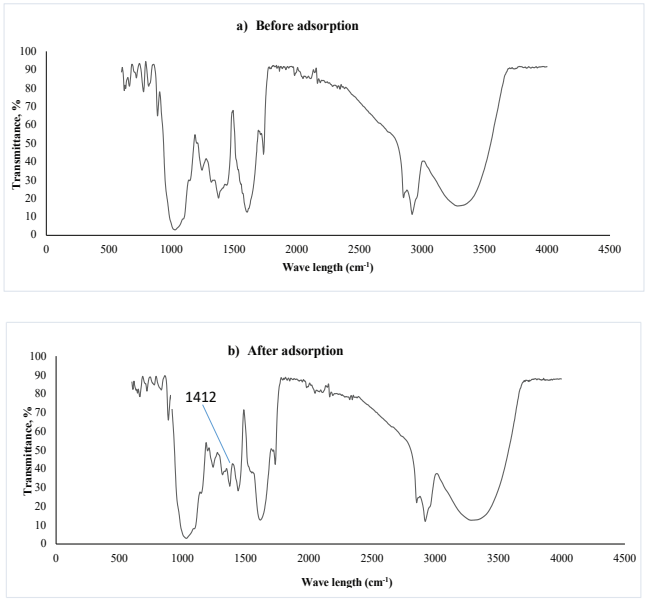

Figure 3: FTIR spectra of the banana peel powder a) before metal adsorption and b) after metal adsorption

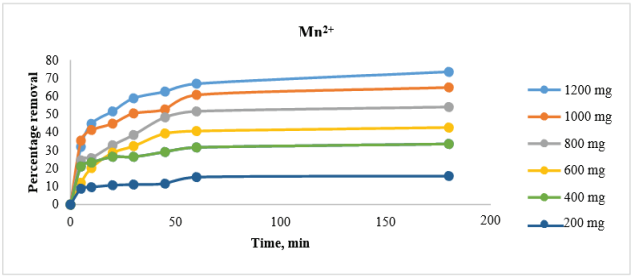

Figure 4: The effects of the mass dosage of banana peel powder on the adsorption of Mn^{2+}

Table 3: Langmuir isotherm parameters

$q_{m(mg/g)}$	6.920
b	0.287
R^2	0.971
R_L	0.080

capacity (q_m) was calculated from equation 1 below, where C_e, mg/l is the equilibrium concentration of the solute, q_e (mg/g) is the amount of metal adsorbed per unit mass of adsorbent at equilibrium, q_m(mg/g) is the maximum adsorption capacity, b (L/g) is a constant related to enthalpy of adsorption.

$$\frac{1}{q_e} = \frac{1}{bq_mC_e} + \frac{1}{q_m} \text{ ----------(1)}$$

The linear plot of Freundlich equation for Mn^{2+} adsorption is also shown in figure 6 and the calculated parameters listed in table 4. The Freundlich isotherm model was also best fitted with experimental data as it shows good correlation coefficient values of 0.951. The linearized Freundlich equation is given by:

Table 4: Freundlich isotherm parameters

K_f	3.742
n	6.743
R^2	0.951

$$\log q_e = \frac{1}{n}\log C_e + \log K_f \text{ ---------(2)}$$

Where C_e, mg/l is the equilibrium concentration of the solute, q_e mg/g) is the amount of metal adsorbed per unit mass of adsorbent at equilibrium, K_f (mol/l) and n are equilibrium constants indicative of the adsorption capacity and adsorption intensity, respectively [18]. n are values between 1 and 10 for this model indicate thermodynamically favourable adsorption [19].

These results suggest that Langmuir and Freundlich isotherms follow a good fit for Mn^{2+} adsorption with banana peel powder. Since the values of RL, and n for Mn^{2+} ion is between 0 and 1, and 1 and 10 respectively, this indicates that the adsorption of these metal ions by banana peel is spontaneous [19].

Langmuir isotherm assumes monolayer coverage on a homogeneous surface with identical adsorption sites however these assumptions are valid for gas adsorption on solid surface. In solution-solid systems, with the hydration forces, mass transport effects the system is much more dynamic and complicated, and obeying the isotherm does not necessarily reflect the validity of the aforementioned assumptions. In this system the isotherm adequacy may be seriously affected by the experimental conditions, in particular, the range of concentration of the solute. While Freundlich isotherm is an empirical model that assumes multilayer adsorption, with random distribution of adsorption heat and affinities over the heterogeneous surface. Langmuir and Freundlich isotherm models may adequately describe the same set of liquid-solid adsorption data at certain concentration ranges, in particular, when the concentration is small and the adsorption capacity of the solid is large enough to make both isotherm equations approach a linear form. These results are in agreement with [20] where both models had a good fit to the data. However, these correlation coefficients are only limited to the degree of freedom of 4, which is arbitrarily chosen for this study.

Effects of solution initial pH: The pH of the solution in contact with the banana peel powder has effects on removing metals. This is because the acidic solution has an influence on both the structure of the banana peel powder and exchange ions. The dependence of the heavy metal adsorption on pH is related to the surface functional groups in the banana peel powder. As stated in subsection Selectivity of the adsorbent in Materials and Methods section, the experiments were conducted by varying the solution pH as follows: 2.0, 3.0 and 5 ± 0.2 for the single component solutions whilst keeping all the other parameters constant.

Figure 6a below shows that the heavy metal removal efficiency improves with the increase in the pH of the solution. This is in agreement with similar study conducted by [21]. The removal efficiency of Mn^{2+} at the pH range of 2.0 to 5.0 increased from 28.24% to 71.78 % respectively. The Mn^{2+} metal start to precipitate at pH above 5 [21], hence the pH studied for adsorption of this heavy metals was below 5. Low pH is inhibiting the adsorption of Mn^{2+} onto banana peel powder; the metal ion may be competing with H^+ ions for binding with the banana peel powder surface functional groups. Figure 7 shows that the

pH of the solution increases during the adsorption, due to buffering effect of the banana peel powder because of its alkalinity.

Effects of particle size: Figure 8 shows that the increase in particle size of banana peel powder results in lower Mn^{2+} removal efficiencies. The removal efficiency is higher at the particle size of 0.15 mm, 72.43 % and lowest at the banana peel powder particle size of 5 mm, 6.63 %. Therefore, smaller particles size shows to be more efficient in heavy metals removal. This is in agreement with the work of [22] conducted on the husk of melon seeds. Smaller particles have large surface area for adsorption than larger particles. However, very fine particles may cause difficulty in solid-liquid separation in batch mode, and significant pressure drops in fixed bed columns [23].

Lagergren pseudo first order and second order plots (Figures 9 and 10): Table 5 and figure 10 show that correlation coefficient values (R^2) are very low for all metals under study, the experimental q_e values does not agree with calculated ones, obtained from the linear plot, this further suggest that the adsorption of Mn^{2+} ions does not follow pseudo first order kinetics.

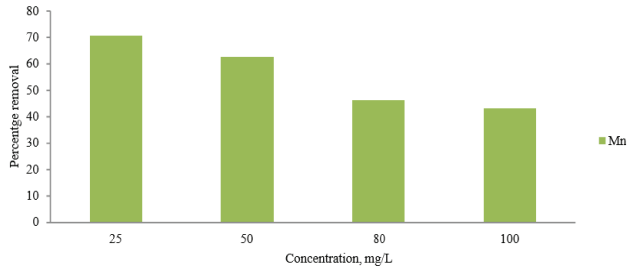

Figure 5: Effects of initial concentration on the adsorption of Mn^{2+}

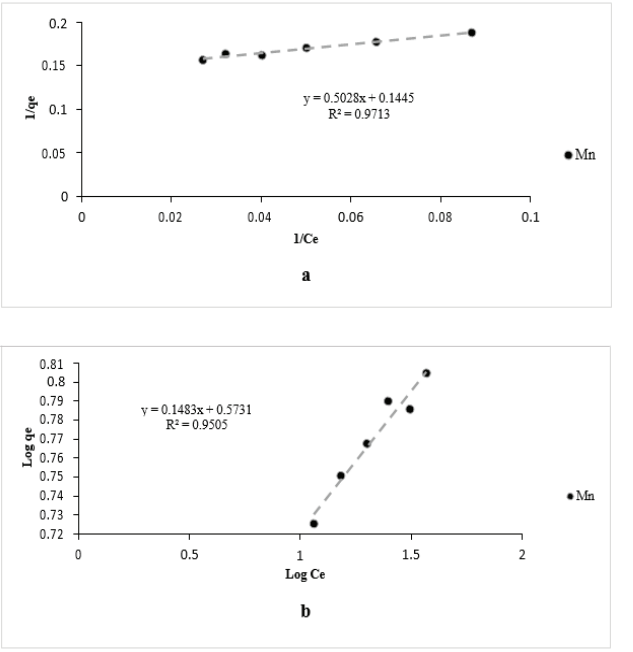

Figure 6: Langmuir (a) and Freundlich (b) linear plot for sorption of Mn^{2+} ions onto banana peel powder

The pseudo-second order rate constant k_2 and q_e values were calculated from the slope and intercept of the plots t/q *vs* t as shown in figure 9. The experimental values of q_e agree well with experimental q_e values. This suggests that the rate-limiting step is chemical sorption that involves valance forces through exchange of electrons between banana peel powder and heavy metals ions, thus the adsorbent exhibited high performance in the adsorption of Al^{3+} and Fe^{3+} ions.

Selectivity of banana peel powder: This section gives the findings and discussion on the use of banana peel powder in adsorption of Mn^{2+} from AMD. Although the metal constituents were not of equal concentration, the adsorbent has shown a great preference to a tri-valent ion than divalent metal ions with the exception of Cd^{2+}, it has removed over 95% of Al^{3+} and Fe^{3+} ions from the solution (Figure 10) and the Fe^{3+} removal efficiency was the close to Cd^{2+} removal at all dosages. The good adsorption of Fe and Al might be because of their high affinity due to their high valence (tri-valence) compared to the competing di-valent metals. This finding is in consistence with the work done by [24].

Column studies-actual acid mine drainage

Effects of bed height: The service time of the column increased with the increase in bed depth as indicated in figure 11 and the adsorption capacity of the bed and saturation time increased with increasing bed depth. This may be attributed to more active sites available for binding and longer mass transfer zone. The analysis and modelling of the column data was done using BDST or Bohrat-Adams equation. This model is one of the simple model used to measures the capacity of the bed at different breakthrough values [25]. However, the model is based on the surface reaction rate theory, and it neglects the film resistance and the intra-particle mass transfer resistance in such that the metal ions are adsorbed directly onto the surface of the adsorbent.

The model states that the bed depth (H) and the service time (t) of the column has a linear relationship, the equation is expressed as:

$$t = \frac{N_0 H}{C_0 v} - \left(\frac{1}{K_a C_0}\right)\ln\left(\frac{C_0}{C_b} - 1\right) \text{-------(3)}$$

where C_0 is the initial concentration of solute (mg/L), C_b is the desired concentration of solute at breakthrough point (mg/L), N_0 is the adsorption capacity (mg/L), H is the bed depth of the column (cm), K_a is the adsorption rate constant l/(mg.min), t is the service time of column(h) and v is the linear flow velocity of feed to bed cm/h.

Setting t=0 yields

$$X_0 = \frac{V}{KC_0}\ln\left(\frac{C_0}{C_b} - 1\right) \text{-------(4)}$$

where X_0 is the minimum column height necessary to achieve an effluent concentration C_b, known as critical bed depth.

Table 5: Kinetics parameters for the adsorption of Mn^{2+} on the banana peel powder

Heavy metal ions	Pseudo-first- order			Pseudo-second-order		
q_e experimental, mg/g	R^2	k_1 (min^{-1})	q_e calculated, mg/g	R^2	k_2 ($g/mg^{-1}.min^{-1}$)	q_e calculated, mg/g
5.634	0.1905	0.005	1.555	0.9978	0.121	5.858

Therefore, the BDST equation can be expressed as

$$t = aH + b \text{ ------(5a)}$$

Where

$$a = slope = \frac{N_0}{C_0 v} \text{ ------(5b)}$$

and

$$b = \text{int}\,ercept = -\frac{1}{K_a C_0}\ln\left(\frac{C_0}{C_b} - 1\right) \text{ -----(5c)}$$

The BDST relation was developed by plotting the data of breakthrough curves for each bed depth of 6, 12.4 and 17.8 cm by recording the service time at 0.2% of initial concentration of each metal ion. Thereafter, the service time (t) was plotted against bed depth (H) at the flow rate of 15 mL/min and was found to be linear as shown in figure 12 below. The breakthrough point where the effluent concentration is approximately 0.2% of the initial concentration intends to achieve compliance to national water standard for discharge of wastewater to watercourse. The discharge standard for Mn is 0.1 mg/L [26]. The validity of the BDST model to present the biosorption of heavy metals ions in this study was indicated by the high correlation coefficient values (R^2=0.991 and R^2=0.996 for Mn and Zn respectively).

From the intercept and the slope of figure 12, the design parameters like N and K_a were found by assuming that the linear flow velocity (v) and concentration (C_o) are constant during the service of the column. The values of N_0K_a, K_a, and X_0 were found to be 133.748 mg/L, 0.103 l/(mg.min) and 2.024 cm for Mn^{2+}, respectively. The rate constant, K_a is a measure of the rate transfer of metal solution from the fluid phase to the solid phase. It influences the breakthrough phenomenon in a column study [27]. When the value of K_a is large the early breakthrough of the bed can be delayed [28]. Therefore, a longer bed depth is recommended for smaller values of K_a to decrease the chances of early breakthrough.

The larger the value of N_0 and smaller value of X_0 indicate high bed capacity for the absorption material. However, the bed capacity will change with service time as the bed depth increases and the residence time with liquid inside the column increases, allowing the adsorbate molecules to diffuse deeper inside the adsorbent.

Table 6 indicates the minimum bed height (X_0) to achieve the desired breakthrough concentration as 2.024 and 0.885 cm for Mn^{2+}. In addition the adsorbent bed exhibited a lower absorption rate constant K_a for Mn^{2+} hence longer bed depth is desired to prevent early breakthrough.

The BDST model parameters are very useful to scale up the process for different flow rates without further laboratory tests. The ratio of the original and the new flowrates can be multiplied by the slope of the plot of service time against bed depth.

The successful design of the adsorption column can also be achieved by using Thomas model to predict the breakthrough profile of the effluent. This model is simple to use and is one of the general and mostly used methods in column performance studies. Thomas model assumes Langmuir kinetics of adsorption-desorption with no axial dispersion and mass transfer kinetics [28,29].

Table 6: The BDST model parameters for the removal of Mn^{2+} on banana peel adsorption bed

Heavy metal ions	K_a (L/(mg.min))	N_o (mg/L)	X_o (cm)	R^2
Mn^{2+}	0.103	133.748	2.024	1

The expression of the Thomas model for an adsorption column is as follows:

$$\frac{C_t}{C_0} = \frac{1}{\left(1 + \exp\left(\frac{K_{TH}}{Q}\left(q_0 M - C_0 V_{eff}\right)\right)\right)} \text{ -------6a}$$

Where C_o is the initial metal ion concentration (mg/L), C_t is the effluent metal ion concentration (mg/L) at any time (t), q_0 is the maximum solid-phase concentration of the solute(mg/g), V_{eff} is the effluent volume (mL), M is the mass of the adsorbent (g), Q is the flow rate mL/min) and KTH is the Thomas rate constant (mL/mg. min).

The linearized form of the Thomas model is as follows:

$$\ln\left(\frac{C_0}{C_t} - 1\right) = \frac{K_{TH} q_0 M}{Q} - \frac{K_{TH} q_0 M}{V_{eff}} \text{ --------6b}$$

Which can be simplified to

$$\ln\left(\frac{C_0}{C_t} - 1\right) = \frac{K_{TH} q_0 M}{Q} - K_{TH} C_0 t \text{ ---------6c}$$

The experimental data was fitted into the Thomas model and the kinetic coefficient KTH and to obtain adsorption capacity of the bed q_o using regression analysis from a plot of $\ln\left(\frac{C_0}{C_t} - 1\right)$ against t at 6, 12.4 and 17.8 cm adsorbent bed and 15 mL/min volumetric flowrate of the influent.

The values of regression coefficient (R^2) are presented in table 7 and are low and the bed adsorption capacity has a random relationship with the bed depth, This indicates that Thomas model is not appropriate for describing the sorption process for Mn^{2+} a banana peel at given conditions. The experimental data did not fit well with the Thomas model. The KTH value decreases with the increase in bed height and is also in agreement with [30] but contradicts the studies by [31].

Effects of flowrates: The effect of the actual AMD flowrate on the adsorption of Mn^{2+} on banana peel adsorbent was studied by varying the influent flowrate (15, 30 and 45 mL/min) with the constant adsorbent bed depth of 17.8 cm, inlet concentration of 46.006 for Mn^{2+}. The Mn^{2+} breakthrough curves in figure 13 shows that at the flowrate of 15 mL/min the adsorption bed take longer to reach breakthrough point (~ 33 minutes) compared to about 15 and 4 minutes taken at flow rates of 30 and 45 mL/min, respectively.

Lower flow rate has resulted in longer residence time of the liquid which allows for more contact time between the metal ions and the adsorbent. However, the high flowrates led to the reduction of metal

Table 7: Thomas model parameters for the removal of Mn^{2+} on banana peel at different bed depths and flow rates of 15 mL/min

Metals	Bed depth (cm)	q_o (mg/g)	K_{TH} (mL/min mg)	R^2
Mn^{2+}	6	5866.500	0.002	0.240
	12.4	2489.913	0.001	0.926
	17.8	2631.586	0.001	0.738

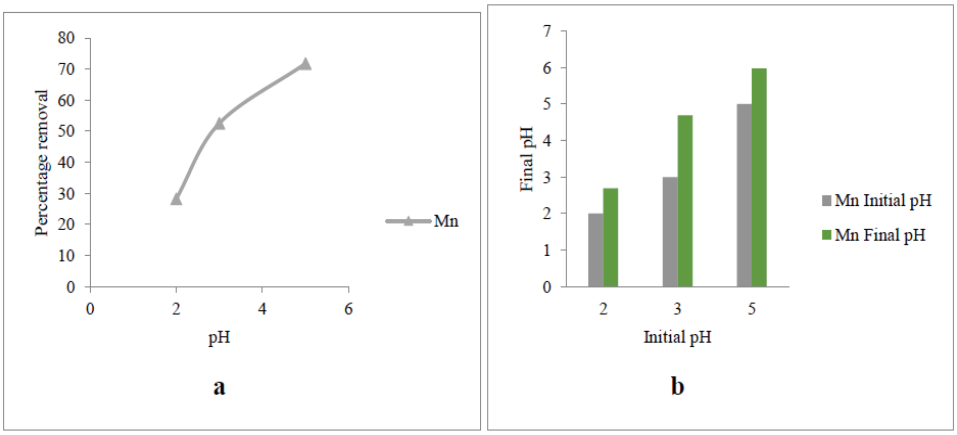

Figure 7: Effects of Initial pH on the percentage removal of Mn^{2+}

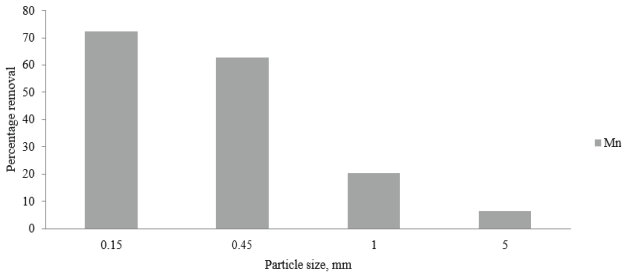

Figure 8: Effects of particle size on the adsorption of Mn^{2+}

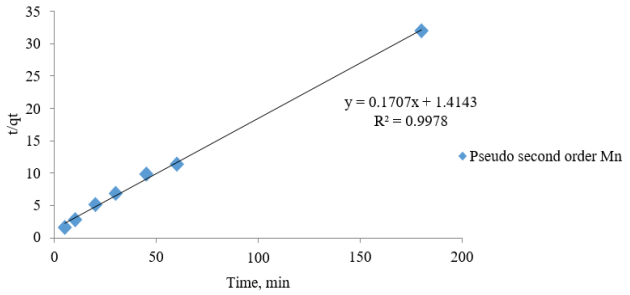

Figure 9: Pseudo second order plot for the adsorption of Mn^{2+}

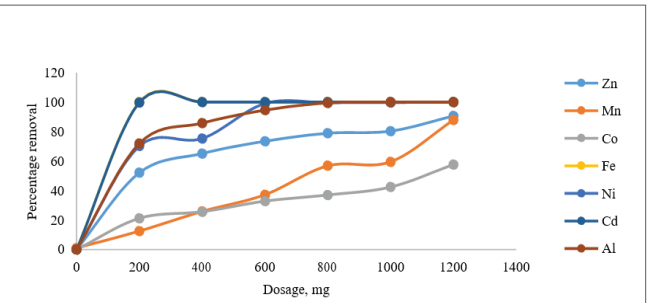

Figure 10: Effects of banana peel powder dosage on adsorption of heavy metals from Actual AMD

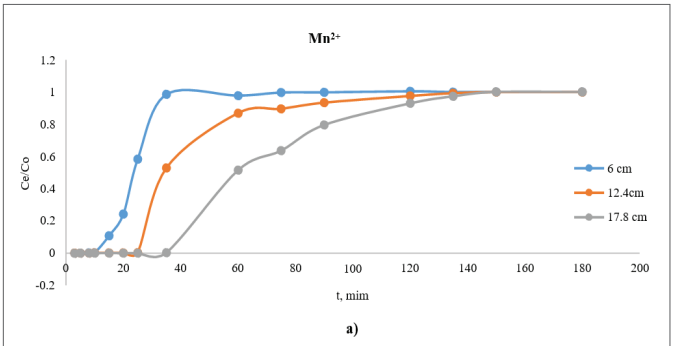

Figure 11: The breakthrough curves of Mn^{2+} removal by banana peel for different bed depth

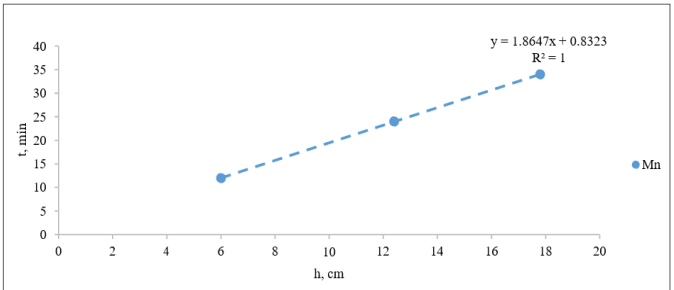

Figure 12: BDST plot for Mn^{2+} at 15 mL/min

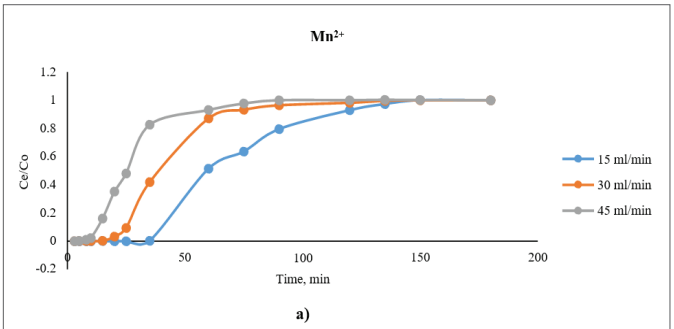

Figure 13: Breakthrough curve for Mn^{2+} removal on different influent flow rate

ion uptake. This reduction is probably due to the unavailability of sufficient contact time for solute to interact with the sorbent and the limited diffusivity of solute into the sorptive sites or pores. This is in agreement with the work done by [32].

The BDST relation was developed by plotting the data of breakthrough curves for each flowrate of 15, 30 and 45 mL/min by recording the service time to reach 0.2% of initial concentration. Thereafter, the service time (t) was plotted against linear velocity at the bed depth of 17.8 cm and was found to be linear as shown in figure 14. The validity of the BDST model to present the biosorption of heavy metals ions in this study was indicated by the high correlation coefficient values (R^2=0.984).

From the intercept and the slope, the design parameters like N_0 and K_a as listed in table 8 were found for the constant bed depth (H) and initial concentration (C_0).

The high correlation coefficient values (R^2=0.984)) indicates the validity of the BDST model to present the removal of heavy metals ion in this study.

The experimental data was fitted to Thomas model by plotting $\ln\left(\frac{C_0}{C_t}-1\right)$ against t at different flow rates (15, 30, 45 mL/min). The relative coefficients and constants were obtained using linear regression analysis from figure 15a, figure 15b and figure 15c, and according to equation 4 the results are listed in table 9.

The results show that q_o values for Mn^{2+} increased with the increase in flow rates, where KTH values were random with each flow rates and depict no trend with the flow rates. The regression coefficient ranges from 0.386 to 0.938.

Conclusion

The main objective of the study was to explore the adsorption potential of banana peels as low cost adsorbent for heavy metals under synthetic water, actual AMD and fortified AMD conditions. The effects of particle size, contact time, mass loading, initial concentration, selectivity and pH were studied. The morphological transformation of the banana peel was also investigated. The metal adsorption of the banana peels from actual AMD was investigated in a fixed bed configuration at different flow rates and bed depths. Banana peels showed that they are capable for removing Mn^{2+} under AMD conditions. The contact time to reach saturation was about 60 minutes. In batch mode the banana peel could remove above 60.70% of Mn^{2+} at the concentration of 43 mg/L of Mn^{2+} in solution, and the percentage removed remained relatively the same in the AMD environment at 59.49%. The adsorption capacity determined by Langmuir for Mn^{2+} metal ions was 6.920 mg/g in the batch mode system. The adsorption percentage of Mn^{2+} increased with the increase in pH.

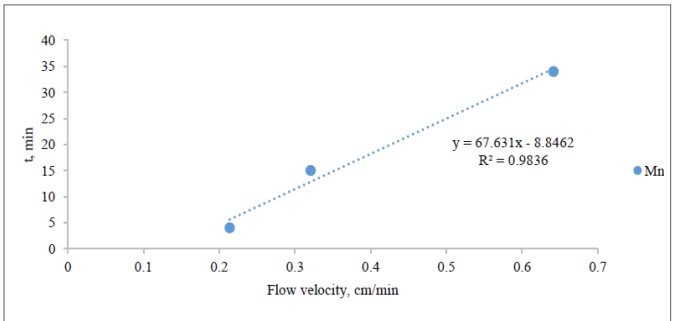

Figure 14: BDST plot for Mn^{2+} at 178 cm

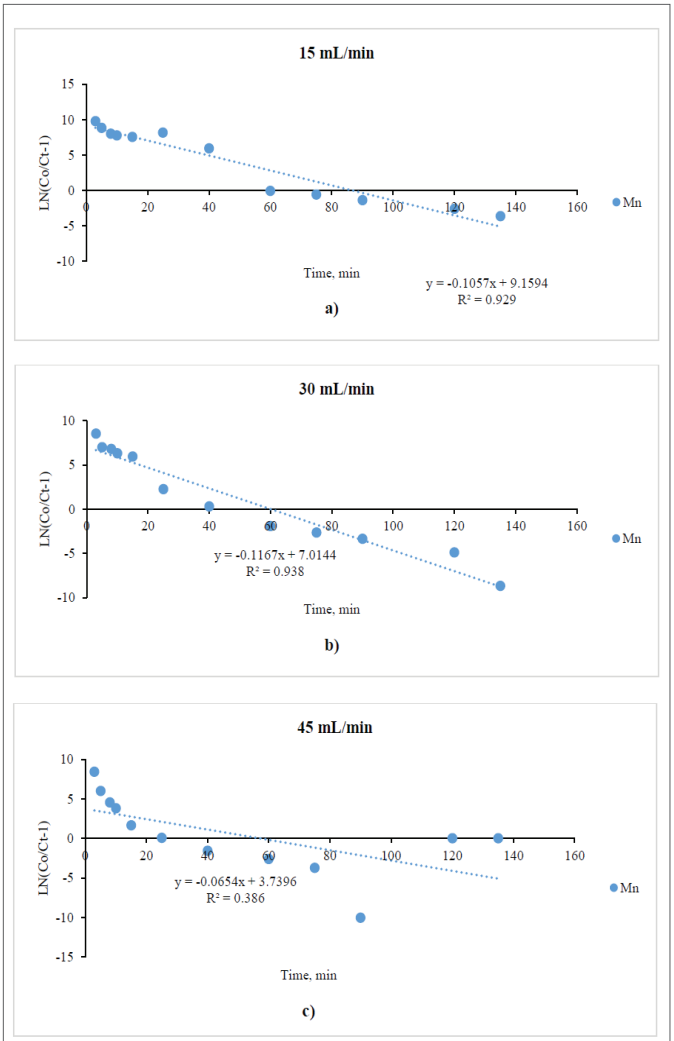

Figure 15: Thomas model plot for the removal of Mn^{2+} on 17.8 cm adsorption bed

Table 8: The BDST model parameters for the removal of Mn^{2+} at 17.8 cm

Heavy metal ions	K_a (L/(mg.min))	N_o (mg/L)	R^2
Mn	0.015	112.132	0.984

Table 9: Thomas model parameters for the removal of Mn^{2+} on banana peel at flow rates and flow rates and 17.8 cm

Metals	Flowrate (mL/min)	q_0 (mg/g)	K_{TH} (mL/min mg)	R^2
Mn	15	1993.318	0.002	0.929
	30	27652.484	0.0003	0.938
	45	3945.964	0.001	0.386

The increase in particle size showed poor adsorption for Mn^{2+} ions. The removal efficiency increased with the increase in mass dosage of the banana peel. The removal efficiency also increased with the increase of the adsorbent bed depth and decreased with the increase in flowrate passing through the bed. The relatively large adsorbent bed depth delayed the breakthrough point owing to more adsorption sites. The relatively high flowrates have quicker breakthrough points; this is attributed to a short contact time of the metal ions with the banana

peel powder. The study showed that the experimental data best fitted BDST model than Thomas model for all conditions tested in this study.

Different bed depth (6, 12.4, 17.8 cm) of banana peel could remove Mn^{2+} to meet the effluent standard of 0.1 mg/L for Mn. The volume of water treated to remove Mn^{2+} from 46.006 mg/L to the effluent standard (0.1 mg/L) at 15 mL/min, through the bed depth of 6, 12.4, and 17.8 cm was 180, 360 and 510 mL, respectively. It can therefore be concluded that banana peel can be used as a cheap adsorbent to remove Mn^{2+} under AMD condition.

References

1. Guj P (2012) Mineral royalties and other mining-specific taxes. International Mining and Development Center, Australia.
2. McCarthy TS (2011) The impact of acid mine drainage in South Africa. S Afr J Sci 107: 1-7.
3. Zhengfu B, Inyang HI, Daniels JL, Frank O, Struthers S (2010) Environmental issues from coal mining and their solutions. Min Sci Technol (China) 20: 215-223.
4. Md Kibria G, Quamruzzaman C, Ullah ASMW, Kabir AKMF (2012) Effect of longwall mining on groundwater for underground coal extraction in Barapukuria, Bangladesh. J Mines Met Fuels 60: 60-66.
5. Coulton R, Bullen C, Dolan J, Hallett C, Wright J, et al. (2003) Wheal Jane mine water active treatment plant- design, construction and operation. Land Contam Reclam 11: 245-252.
6. Taylor J, Pape S, Murphy N (2005) A summary of passive and active treatment technologies for acid and metalliferous drainage (AMD). 5th Australian workshop on Acid Mine Drainage, Fremantle, Australia.
7. Johnson DB, Hallberg KB (2005) Acid mine drainage remediation options: a review. Sci Total Environ 338: 3-14.
8. da Silveira AN, Silva R, Rubio J (2009) Treatment of Acid Mine Drainage (AMD) in South Brazil: Comparative active processes and water reuse. Int J Miner Process 93: 103-109.
9. Bajpai AK, Rajpoot M (1999) Adsorption Techniques-A Review. J Sci Ind Res 58: 884-860.
10. Montanher SF, Oliveira EA, Rollemberg MC (2005) Removal of metal ions from aqueous solutions by sorption onto rice bran. J Hazard Mater 117: 207-211.
11. Mavrov V, Stamenov S, Todorova E, Chmiel H, Erwe T (2006) New hybrid electrocoagulation membrane process for removing selenium from industrial wastewater. Desalination 201: 290-296.
12. Al-Azzawi MNA, Shartooh SM, Al-Hiyaly SAK (2013) The removal of zinc, chromium and nickel from industrial waste water using banana peels. Iraqi J Sci 54: 72-81.
13. Chao HP, Chang CC, Nieva A (2014) Biosorption of heavy metals on *Citrus maxima* peel, passion fruit shell, and sugarcane bagasse in a fixed-bed column. J Ind Eng Chem 20: 3408-3414.
14. El-Sayed GO, Dessouki HA, Ibrahiem SS (2011) Removal of Zn (II), Cd (II) and Mn (II) from aqueous solutions by adsorption on maize stalks. Malays J Anal Sci 15: 8-21.
15. Zhang Y, Zhao J, Jiang Z, Shan D, Lu Y (2014) Biosorption of Fe (II) and Mn (II) ions from aqueous solution by rice husk ash. Biomed Res Int 2014: 973095.
16. Iqbal M, Edyvean RGJ (2004) Biosorption of lead, copper and zinc ions on loofa sponge immobilized biomass of *Phanerochaete chrysosporium*. Miner Eng 17: 217-223.
17. Al-Asheh S, Duvnjak Z (1995) Adsorption of copper and chromium by *Aspergillus carbonarius*. Biotechnol Prog 11: 638-642.
18. Veli S, Alyuz B (2007) Adsorption of copper and zinc from aqueous solutions by using natural clay. Journal of hazardous materials 149: 226-233.
19. Falayi T, Ntuli F (2014) Removal of heavy metals and neutralisation of acid mine drainage with un-activated attapulgite. J Ind Eng Chem 20: 1285-1292.
20. Anwar J, Shafique U, Waheed-uz-Zaman, Salman Md, Dar A, et al. (2010) Removal of Pb (II) and Cd (II) from water by adsorption on peels of banana. Bioresour Technol 101: 1752-1755.
21. Wu Y, Zhou J, Wen Y, Jiang L, Wu Y (2012) Biosorption of heavy metal ions (Cu^{2+}, Mn^{2+}, Zn^{2+}, and Fe^{3+}) from aqueous solutions using activated sludge: Comparison of aerobic activated sludge with anaerobic activated sludge. Appl Biochem Biotechnol 168: 2079-2093.
22. Giwa AA, Bello IA, Oladipo MA, Adeoye DO (2013) Removal of cadmium from waste-water by adsorption using the husk of melon (*Citrullus lanatus*) Seed. Int J Sci Basic Appl Sci 2: 110-123.
23. Inglezakis VJ, Lemonidou M, Grigoropoulou HP (2001) Liquid holdup and flow dispersion in zeolite packed beds. Chem Eng Sci 56: 5049-5057.
24. Kang SY, Lee JU, Moon SH, Kim KW (2004) Competitive adsorption characteristics of Co^{2+}, Ni^{2+}, and Cr^{3+} by IRN-77 cation exchange resin in synthesized wastewater. Chemosphere 56: 141-147.
25. Vimala R, Charumathi D, Das N (2011) Packed bed column studies on Cd (II) removal from industrial wastewater by macrofungus *Pleurotus platypus*. Desalination 275: 291-296.
26. Department of Water Affairs (2013) Revision of general authorisations in terms of Section 39 of the National Water Act, 1998 (Act No. 36 of 1998). Government Gazette.
27. Simate GS, Ndlovu S (2015) The removal of heavy metals in a packed bed column using immobilized cassava peel waste biomass. J Ind Eng Chem 21: 635-643.
28. Vijayaraghavan K, Jegan J, Palanivelu K, Velan M (2005) Batch and column removal of copper from aqueous solution using a brown marine alga *Turbinaria ornate*. Chem Eng J 106: 177-184.
29. Fu Y, Viraraghavan T (2003) Column studies for biosorption of dyes from aqueous solutions on immobilised *Aspergillus niger* fungal biomass. Water SA 29: 465-472.
30. Chen S, Yue Q, Gao B, Li Q, Xu X, et al. (2012) Adsorption of hexavalent chromium from aqueous solution by modified corn stalk: a fixed-bed column study. Bioresour Technol 113: 114-120.
31. Chowdhury ZZ, Zain SM, Rashid AK, Rafique RF, Khalid K (2012) Breakthrough curve analysis for column dynamics sorption of Mn (II) ions from wastewater by using *Mangostana garcinia* peel-based granular-activated carbon. J Chem 2013: 1-8.
32. Hasfalina CM, Maryam RZ, Luqman CA, Rashid M (2012) Adsorption of copper (II) from aqueous medium in fixed-bed column by kenaf fibres. APCBEE Procedia 3: 255-263.